



Hill, R. A. and Sutherland, A. (2018) Hot off the press. *Natural Product Reports*, 35(10), pp. 1024-1028.

There may be differences between this version and the published version. You are advised to consult the publisher's version if you wish to cite from it.

<http://eprints.gla.ac.uk/170043/>

Deposited on: 15 November 2018

Enlighten – Research publications by members of the University of Glasgow_
<http://eprints.gla.ac.uk>

Hot off the Press

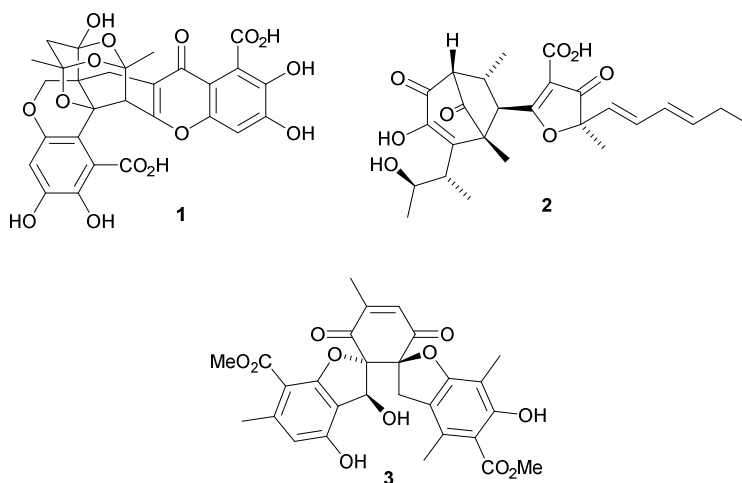
Robert A. Hill and Andrew Sutherland

School of Chemistry, Glasgow University, Glasgow, UK, G12 8QQ.

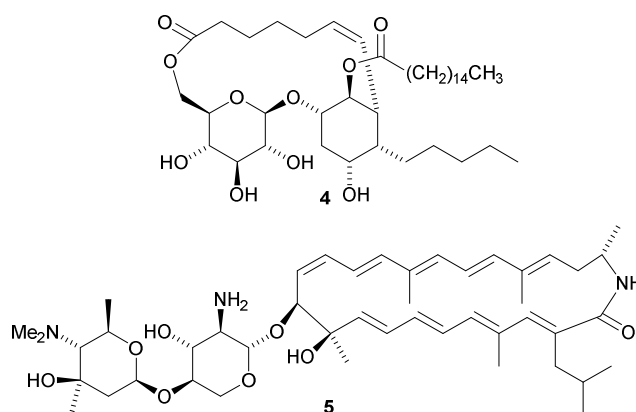
E-mail: Bob.Hill@glasgow.ac.uk, Andrew.Sutherland@glasgow.ac.uk

Abstract: A personal selection of 32 recent papers is presented covering various aspects of current developments in bioorganic chemistry and novel natural products such as hyperphlegmine A from *Huperzia phlegmaria*.

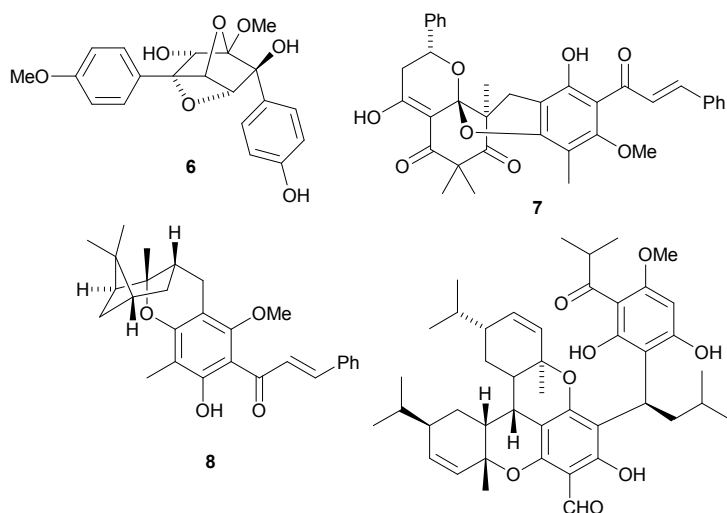
The structure of citrofulvicin **1**, a racemic metabolite from *Penicillium velutinum*, was confirmed by X-ray analysis.¹ It is proposed that the unprecedented framework of citrofulvicin **1** is formed by nonenzymatic Diels-Alder cycloaddition between heptaketide precursors. The structure of asperone A **2**, a metabolite of *Aspergillus* sp. AWG 1-15, was established by X-ray analysis of a methylated derivative.² A biosynthetic pathway to asperone A **2**, involving two polyketide precursors, has been suggested. The structure of tsavoenone A **3**, from the lichen *Parmotrema tsavoense*, was also established by X-ray analysis.³ A putative biosynthetic scheme for the formation of tsavoenone A **3** from a depsidone precursor, parmosidone D, has been presented.



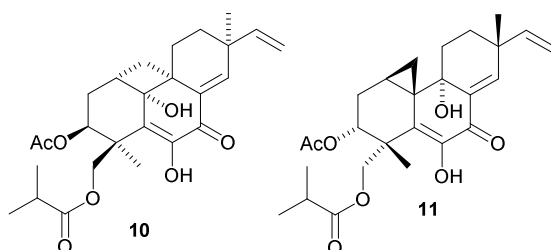
The insect-borne fungus *Mucor* sp. SNB-VECD13A produces mucorolactone **4** with a novel macrolactone skeleton that may be derived from linoleic acid.⁴ Activation of a silent biosynthetic gene cluster in *Streptomyces roseosporus* produces a polyketide macrolactam, auroramycin **5**, that shows potent antibiotic activity.⁵ Auroramycin **5** contains an unusual isobutyl extender unit and a novel disaccharide.

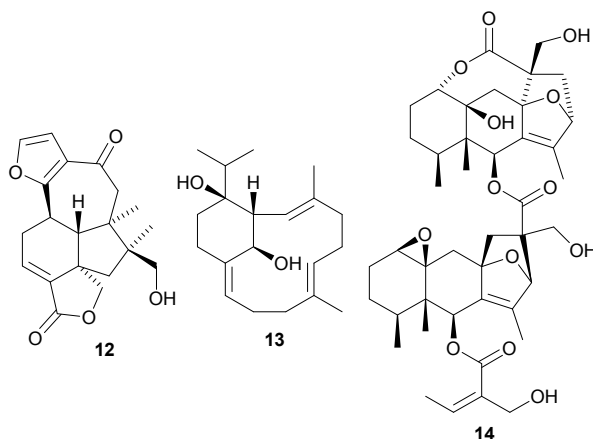


Four highly oxygenated *p*-terphenyl derivatives, including hawaiiinol A **6**, have been identified as metabolites of the insect-associated fungus *Paraconiothyrium hawaiiense*.⁶ Hawaiiinol A **6** is the first example of a terphenyl with a 4,7-dioxatricyclo[3.2.1.0^{3,6}]octane unit and its structure and absolute configuration were determined by X-ray analysis. Further unusual natural products whose structures have been confirmed by X-ray analyses include cleistoperlones A **7** and C **8**, from *Cleistocalyx operculatus*,⁷ and eucalyptusdimer A **9**, from *Eucalyptus robusta*.⁸ Cleistoperlone A **7** is formed from two cinnamylphloroglucinol units and cleistoperlone C **8**, from a cinnamylphloroglucinol unit with α -pinene. Eucalyptusdimer A **9** has an unprecedented skeleton featuring two phelandrene and two acylphloroglucinol units. Biosynthetic pathways have been proposed for cleistoperlones A **7** and C **8** and eucalyptusdimer A **9**.

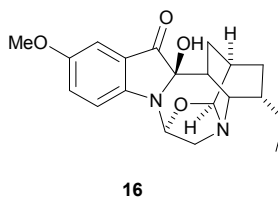
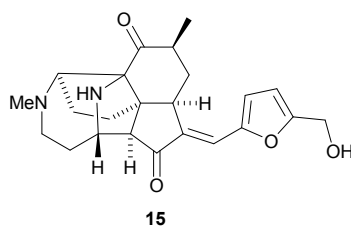


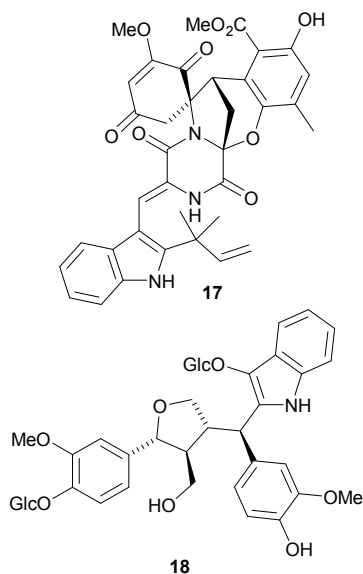
A rearranged isopimarane diterpenoid derivative featuring a fused cyclobutane ring, eutypellenone A **10**, is a metabolite of *Eutypella* sp. D-1.⁹ The authors claim that eutypellenone A **10** belongs to the opposite enantiomeric series as the cometabolite libertellenone H **11**. Salvifarinin A **12**, from *Salvia farinacea*, has a cyclised and rearranged clerodane skeleton.¹⁰ The authors propose a biosynthetic pathway to salvifarinin A **12** which is supported by a biomimetic synthesis. Mangelonoid A **13**, from *Croton mangelong*, has a novel 2,20-cyclocembrane diterpenoid skeleton.¹¹ The structures of salvifarinin A **12** and mangelonoid A **13** were confirmed by X-ray analyses. Four eremophilane sesquiterpenoid dimers and trimers, such as ligusaginoid A **14**, have been isolated from *Ligularia sagitta*.¹² A biosynthetic pathway to ligusaginoid A **14** has been proposed involving two Diels-Alder cycloadditions.



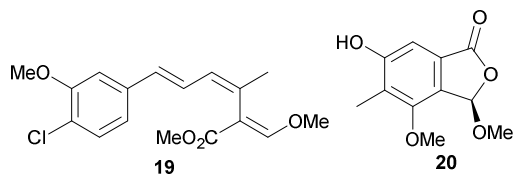


Huperphlegmine A **15**, from *Huperzia phlegmaria*,¹³ and erchinine A **16**, from *Ervatamia chinensis*,¹⁴ have new alkaloid skeletons. Biosynthetic pathways from obscurinine to huperphlegmine A **15** and from ibogaine to erchinine A **16** have been proposed. The structure of the racemic spirocyclic diketopiperazine valiecolortin A **17**, from the marine-derived fungus *Eurotium* sp. SCSIO F452, was established by X-ray analysis.¹⁵ A biosynthetic pathway to the novel skeleton of valiecolortin A **17** has been suggested involving a hetero-Diels-Alder cycloaddition of a diketopiperazine with an anthraquinone and a Baeyer-Villiger oxidation as key steps. Isatindolignanose A **18**, from roots of *Isatis indigotica*, is the first report of an indole linked to a lignan.¹⁶ The authors propose a biosynthetic pathway to isatindolignanose A **18**.



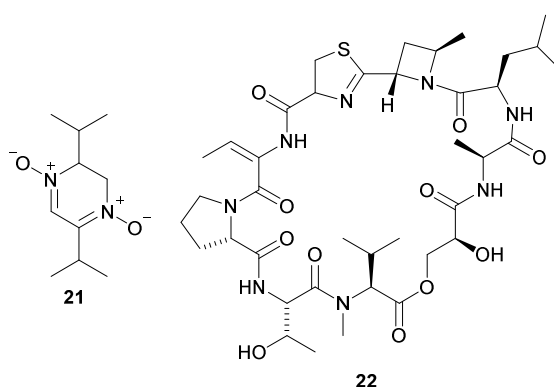


Feeding studies have been used to investigate the biosynthesis of strobilurins (e.g. strobilurin B **19**), antifungal metabolites isolated from various basidiomycetes.¹⁷ These studies have shown that the strobilurins are formed from a linear tetraketide and a benzoate starter unit, which is produced from phenylalanine via cinnamate. The isolation of a novel biphenyl metabolite, pseudostrobilurin B confirmed the involvement of an epoxide intermediate during the formation of the β -methoxyacrylate moiety. Disruption of LaeB, a global regulator from *Aspergillus nidulans* has allowed activation of secondary metabolism and the isolation of eight cryptic compounds.¹⁸ These include seven polyketides such as 3-methoxyporriolide **20**, an optically active phthalide.

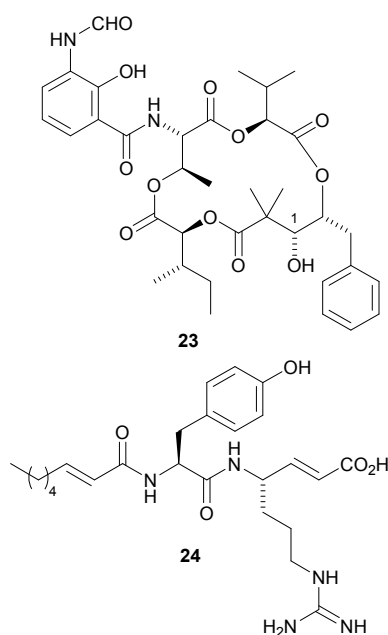


Genome mining in *Pseudomonas* and overexpression of the *Pseudomonas virulence factor* (*pvf*) gene cluster has allowed the isolation of a family of pyrazine *N*-oxides, including the novel dihydropyrazine *N,N'*-dioxide **21**.¹⁹ Following characterisation of the nonribosomal peptide synthetase (NRPS) responsible for the formation of these

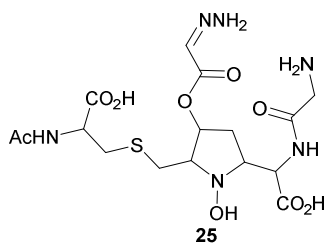
compounds, a biosynthetic pathway from valine has been proposed. The biosynthetic gene cluster from the myxobacterium *Cystobacter violaceus* Cb vi35 that produces vioprolides (e.g. vioprolide C **22**), anticancer and antifungal compounds has been identified.²⁰ As well as the expression of the gene cluster in a stable heterologous host, which allowed high-titre production of these compounds, further studies revealed an *S*-adenosylmethionine (SAM)-dependent enzyme and a methyltransferase involved in the formation of the 4-methylazetidinecarboxylic acid moiety.

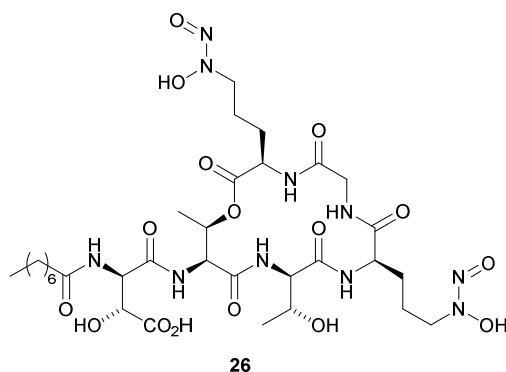


Genome sequencing and bioinformatics analysis has identified the biosynthetic gene cluster of antimycin-type depsipeptides from *Streptomyces conglobatus* such as neoantimycin A **23**, which have significant anticancer activities.²¹ Heterologous expression of the partial gene cluster in *Streptomyces albus* J1074 led to the production of **23**, while bioengineering revealed an NADPH-dependent reductase responsible for formation of the C-1 hydroxyl. A unique NRPS-polyketide synthase hybrid gene cluster from *Sulfurospirillum barnesii* has been analysed and following gene expression and comparative metabolomics, led to the isolation of the lipodipeptide, barnesin A **24**.²² The structure of barnesin A **24** was confirmed by total synthesis and the compound was found to have antimicrobial activity, as well as being a selective inhibitor of cathepsin B.

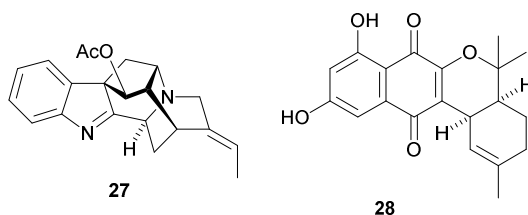


Further characterisation of the biosynthetic gene cluster from *Streptomyces* sp. SoC090715LN-17, that produces s56-p1 **25**, a dipeptide with a unique hydrazine unit has allowed the characterisation of three new enzymes.²³ A combination of in vivo and in vitro experiments has shown that these enzymes cooperate to form the hydrazinoacetic acid component of s56-p1. Genome mining and analysis of *Paraburkholderia graminis* has led to the characterisation of gramibactin **26**, an iron binding lipodepsipeptide.²⁴ NMR spectroscopy and in particular, complexation-induced chemical shifts were used to show that the *N*-nitrosohydroxylamine moieties are involved in metal binding.



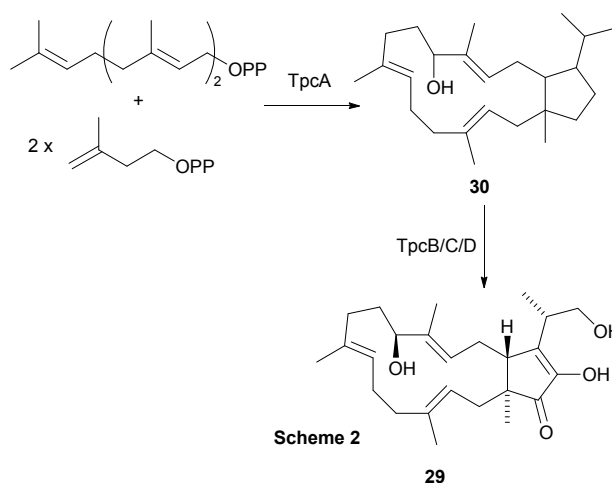
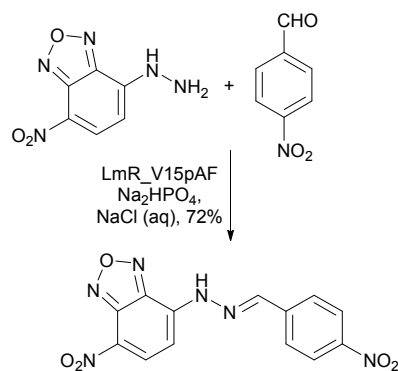


Three homologous cytochrome P450 enzymes from three indole alkaloid-producing plants have been discovered and shown to allow entry to two distinct classes of alkaloids, the sarpagans (e.g. vinorine **27**) and the β -carbolines.²⁵ These results reveal via a common mechanism, how distinct substrates lead to either a cyclisation or aromatisation process. The biosynthetic pathway of marinone and naphterpin natural products such as naphthgeranine A **28** have been shown to involve a cryptic halogenation, mediated by vanadium-dependent chloroperoxidase (VCPO) enzymes.²⁶ The VCPO-catalysed transformation involves a dearomatisation and dichlorination, followed by an α -hydroxyketone rearrangement and loss of chloride anion leaving groups, resulting in the highly oxidised naphthoquinone core.



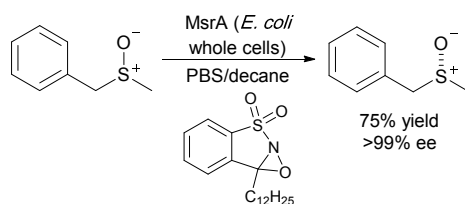
An artificial enzyme that has the ability to catalyse hydrazine (Scheme 1) and oxime formation has been created.²⁷ Introduction of the catalytically active *p*-aminophenylalanine into a promiscuous binding pocket of the multidrug transcriptional regulator from *Lactococcus lactis* results in a designer enzyme that can outperform other catalysts such as aniline. Heterologous expression of four enzymes (*tpcA–D*) in *Aspergillus oryzae* has allowed the total biosynthesis of the sesterterpene,

(-)-terpestacin **29**.²⁸ Following formation of preterpestacin I **30** by terpene synthase TpcA, three hydroxyl groups are introduced by two cytochrome P450 enzymes (TpcB/C) (Scheme 2). The process is then completed by the flavin-dependent oxidase TpcD, which catalyses oxidation of a diol unit to generate (-)-terpestacin **29**.

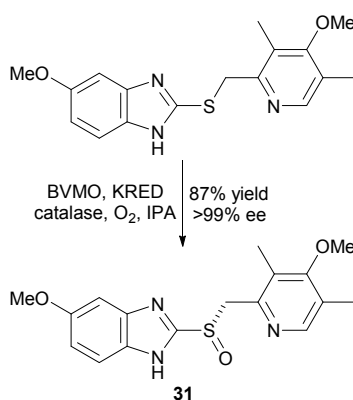


The first biocatalytic deracemisation of sulfoxides has been achieved using a combination of an oxaziridine-type oxidant and the highly enantioselective methionine sulfoxide reductase A (MsrA).²⁹ A biphasic system was used in which MsrA performs a kinetic resolution, forming a sulfide that is oxidised back to the sulfoxide by the oxaziridine-based lipophilic oxidant (Scheme 3). Overall, the process showed a wide substrate scope, producing optically active sulfoxides with excellent enantioselectivity. A combination of air as the terminal oxidant and an engineered Baeyer-Villiger monooxygenase (BVMO) has been used for the preparation of the

chiral sulfoxide, esomeprazole **31**, the *S*-enantiomer and active pharmaceutical ingredient of the blockbuster drug Nexium.³⁰ By directed evolution, the resulting engineered BVMO mediated-process provides an alternative to the Kagan chemocatalytic oxidation, producing esomeprazole in 87% yield and in >99% enantiomeric excess (Scheme 4).

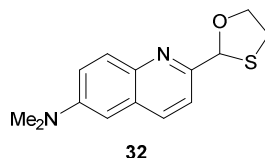
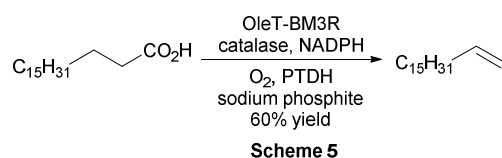


Scheme 3



Scheme 4

A self-sufficient protein, OleT-BM3R, formed from the fusion of the decarboxylase OleT_{JE} and the reductase domain of P450BM3 has been shown to catalyse the oxidative decarboxylation of carboxylic acids to form linear α -olefins.³¹ The engineered fusion protein uses oxygen as the oxidant and NADPH as the electron donor, and in combination with a phosphite dehydrogenase-based NADPH regeneration system (Scheme 5), gave product titres of up to 2.51 g L⁻¹. A quinolone-based two-photon fluorescent probe **32** has been developed for the ratiometric detection and imaging of hypochlorous acid (HClO).³² In response to HClO, the probe shows a decrease in blue emission with a concurrent increase of green emission and was used for detecting exogenous and endogenous HClO in living cells.



References

- 1 Y. Chen, N. Jiang, Y. J. Wei, X. Li, H. M. Ge, R. H. Jiao and R. X. Tan, *Org. Lett.*, 2018, **20**, 3741.
- 2 G.-P. Yin, Y.-R. Wu, C. Han, X.-B. Wang, H.-L. Gao, Y. Yin, L.-Y. Kong and M.-H. Yang, *Org. Chem. Front.*, 2018, **5**, 2432.
- 3 T.-H. Duong, M. A. Beniddir, G. Genta-Jouve, T. Aree, M. Chollet-Krugler, J. Boustie, S. Ferron, A. Sauvager, H.-H. Nguyen, K.-P.-P. Nguyen, W. Chavasiri and P. L. Pogam, *Org. Biomol. Chem.*, 2018, **16**, 5913.
- 4 S. Touré, M. Barthélémy, J. Sorres, G. Genta-Jouve, I. Dusfour, V. Eparvier and D. Stien, *Org. Lett.*, 2018, **20**, 3780.
- 5 Y. H. Lim, F. T. Wong, W. L. Yeo, K. C. Ching, Y. W. Lim, E. Heng, S. Chen, D.-J. Tsai, T.-L. Lauderdale, K.-S. Shia, Y. S. Ho, S. Hoon, E. L. Ang, M. M. Zhang and H. Zhao, *ChemBioChem*, 2018, **19**, 1716.
- 6 F. Ren, S. Chen, Y. Zhang, S. Zhu, J. Xiao, X. Liu, R. Su and Y. Che, *J. Nat. Prod.*, 2018, **81**, 1752.
- 7 J.-C. Su, S. Wang, W. Cheng, X.-J. Huang, M.-M. Li, R.-W. Jiang, Y.-L. Li, L. Wang, W.-C. Ye and Y. Wang, *J. Org. Chem.*, 2018, **83**, 8522.
- 8 X.-J. Qin, M.-Y. Feng, H. Liu, W. Ni, T. Rauwolf, J. A. Porco, Jr., H. Yan, L. He and H.-Y. Liu, *Org. Lett.*, 2018, **20**, 5066.

- 9 H.-B. Yu, X.-L. Wang, Y.-X. Zhang, W.-H. Xu, J.-P. Zhang, X.-Y. Zhou, X.-L. Lu, X.-Y. Liu and B.-H. Jiao, *J. Nat. Prod.*, 2018, **81**, 1553.
- 10 M. Fan, X.-J. Chen, X.-D. Wu, L.-D. Shao, X. Ji and Q.-S. Zhao, *Tetrahedron Lett.*, 2018, **59**, 3065.
- 11 W.-Y. Zhang, J.-X. Zhao, L. Sheng, Y.-Y. Fan, J.-Y. Li, K. Gao and J.-M. Yue, *Org. Lett.*, 2018, **20**, 4040.
- 12 H.-Y. Li, Z.-Q. Zheng, W.-J. Wei, J.-J. Chen and K. Gao, *Tetrahedron Lett.*, 2018, **59**, 3461.
- 13 H. T. Nguyen, H. T. Doan, D. V. Ho, K. T. Pham, A. Raal and H. Morita, *Fitoterapia*, 2018, **129**, 267.
- 14 H.-F. Yu, X.-J. Qin, C.-F. Ding, X. Wei, J. Yang, J.-R. Luo, L. Liu, A. Khan, L.-C. Zhang, C.-F. Xia and X.-D. Luo, *Org. Lett.*, 2018, **20**, 4116.
- 15 W. Zhong, J. Wang, X. Wei, Y. Chen, T. Fu, Y. Xiang, X. Huang, X. Tian, Z. Xiao, W. Zhang, S. Zhang, L. Long and F. Wang, *Org. Lett.*, 2018, **20**, 4593.
- 16 L. Meng, Q. Guo, M. Chen, J. Jiang, Y. Li and J. Shi, *Chin. Chem. Lett.*, 2018, **29**, 1257.
- 17 Z. Iqbal, L.-C. Han, A. M. Soares-Sello, R. Nofiani, G. Thormann, A. Zeeck, R. J. Cox, C. L. Willis and T. J. Simpson, *Org. Biomol. Chem.*, 2018, **16**, 5524.
- 18 H. Lin, H. Lyu, S. Zhou, J. Yu, N. P. Keller, L. Chen and W.-B. Yin, *Org. Biomol. Chem.*, 2018, **16**, 4973.
- 19 A. M. Kretsch, G. L. Morgan, J. Tyrrell, E. Mevers, I. Vallet-Gély and B. Li, *Org. Lett.*, 2018, **20**, 4791.
- 20 F. Yan, D. Auerbach, Y. Chai, L. Keller, Q. Tu, S. Hüttel, A. Glemser, H. A. Grab, T. Bach, Y. Zhang and R. Müller, *Angew. Chem. Int. Ed.*, 2018, **57**, 8754.

- 21 Y. Zhou, X. Lin, S. R. Williams, L. Liu, Y. Shen, S.-P. Wang, F. Sun, S. Xu, H. Deng, P. F. Leadlay and H.-W. Lin, *ACS Chem. Biol.*, 2018, **13**, 2153.
- 22 M. Rischer, L. Raguž, H. Guo, F. Keiff, G. Diekert, T. Goris and C. Beemelmans, *ACS Chem. Biol.*, 2018, **13**, 1990.
- 23 K. Matsuda, T. Tomita, K. Shin-ya, T. Wakimoto, T. Kuzuyama and M. Nishiyama, *J. Am. Chem. Soc.*, 2018, **140**, 9083.
- 24 R. Hermenau, K. Ishida, S. Gama, B. Hoffmann, M. Pfeifer-Leeg, W. Plass, J. F. Mohr, T. Wichard, H.-P. Saluz and C. Hertweck, *Nat. Chem. Biol.*, 2018, **14**, 841.
- 25 T.-T. T. Dang, J. Franke, I. Soares, T. Carqueijeiro, C. Langley, V. Courdavault and S. E. O'Connor, *Nat. Chem. Biol.*, 2018, **14**, 760.
- 26 L. A. M. Murray, S. M. K. McKinnie, H. P. Pepper, R. Erni, Z. D. Miles, M. C. Cruickshank, B. López-Pérez, B. S. Moore and J. H. George, *Angew. Chem. Int. Ed.*, 2018, **57**, 11009.
- 27 I. Drienovská, C. Mayer, C. Dulson and G. Roelfes, *Nat. Chem.*, 2018, **10**, 946.
- 28 K. Narita, A. Minami, T. Ozaki, C. Liu, M. Kodama and H. Oikawa, *J. Org. Chem.*, 2018, **83**, 7042.
- 29 V. Nosek and J. Míšek, *Angew. Chem. Int. Ed.*, 2018, **57**, 9849.
- 30 Y. K. Bong, S. Song, J. Nazor, M. Vogel, M. Widegren, D. Smith, S. J. Collier, R. Wilson, S. M. Palanivel, K. Narayanaswamy, B. Mijts, M. D. Clay, R. Fong, J. Colbeck, A. Appaswami, S. Muley, J. Zhu, X. Zhang, J. Liang and D. Entwistle, *J. Org. Chem.*, 2018, **83**, 7453.
- 31 C. Lu, F. Shen, S. Wang, Y. Wang, J. Liu, W.-J. Bai and X. Wang, *ACS Catal.*, 2018, **8**, 5794.

32 Z. Mao, M. Ye, W. Hu, X. Ye, Y. Wang, H. Zhang, C. Li and Z. Liu, *Chem. Sci.*,
2018, **9**, 6035.